HHS Public Access

Author manuscript

J Biomater Sci Polym Ed. Author manuscript; available in PMC 2020 August 25.

Published in final edited form as:

J Biomater Sci Polym Ed. 2018 September ; 29(13): 1625–1642. doi:10.1080/09205063.2018.1479084.

Combining Electrospun Nanofibers with Cell-Encapsulating Hydrogel Fibers for Neural Tissue Engineering

Ryan J. Miller[a], **Cheook Y. Chan**[a,b], **Arjun Rastogi**[a], **Allison M. Grant**[a,b], **Christina M. White**[a], **Nicole Bette**[a], **Nicholas J. Schaub**[a,c], **Joseph M. Corey**[a,c,d,e,f,*]

[a]Department of Research and Geriatric Research Education and Clinical Center (GRECC), VA Ann Arbor Healthcare System, Ann Arbor, Michigan 48105

[b]Undergraduate Research Opportunity Program, The University of Michigan, Ann Arbor, MI 48109, USA

[c]Department of Neurology, The University of Michigan, Ann Arbor, MI 48109, USA

[d]Department of Biomedical Engineering, The University of Michigan, Ann Arbor, MI 48109, USA

[e]Macromolecular Science and Engineering Program, The University of Michigan, Ann Arbor, MI 48109, USA

[f]Neuroscience Graduate Program, The University of Michigan, Ann Arbor, MI 48109, USA

Abstract

A promising component of biomaterial constructs for neural tissue engineering are electrospun fibers, which differentiate stem cells and neurons as well as direct neurite growth. However, means of protecting neurons, glia, and stem cells seeded on electrospun fibers between lab and surgical suite have yet to be developed. Here we report an effort to accomplish this using cell-encapsulating hydrogel fibers made by interfacial polyelectrolyte complexation (IPC). IPC-hydrogel fibers were created by interfacing acid-soluble chitosan (AsC) and cell-containing alginate and spinning them on bundles of aligned electrospun fibers. Primary spinal astrocytes, cortical neurons, or L929 fibroblasts were mixed into alginate hydrogels prior to IPC-fiber spinning. The viability of each cell type was assessed at 30 min, 4 h, 1 d, and 7 d after encapsulation in IPC hydrogels.. Some neurons were encapsulated in IPC-hydrogel fibers made from water-soluble chitosan (WsC). Neurons were also stained with Tuj1 and assessed for neurite extension. Neuron survival in AsC-fibers was worse than astrocytes in AsC-fibers ($p<0.05$) and neurons in WsC-fibers ($p<0.05$). As expected, neuron and glia survival was worse than L929 fibroblasts ($p<0.05$).Neurons in IPC-hydrogel fibers fabricated with WsC extended neurites robustly, while none in AsC fibers did. Neurons remaining inside IPC-hydrogel fibers extended neurites inside them, while others de-encapsulated, extending neurites on electrospun fibers, which did not fully integrate with IPC-hydrogel fibers. This study demonstrates that primary neurons and astrocytes can be encapsulated in IPC-hydrogel fibers at good percentages of survival. IPC

*Corresponding Author Joseph M. Corey, MD, PhD, Associate Professor, Department of Neurology, University of Michigan, Asst. Chief and Dir. Neurology Education, VA Ann Arbor Healthcare Center, Research (151), 2215 Fuller Rd., Ann Arbor, MI 48105, Phone 734-845-3072, Fax 734-845-3298, coreyj@umich.edu.

hydrogel technology may be a useful tool for encapsulating neural and other cells on electrospun fiber scaffolds.

Keywords

interfacial polyelectrolyte complexation; neuron; neurite; hydrogel; electrospinning

Introduction

Millions are affected by nervous system injury, whether to the brain (1), spinal cord (2), or peripheral nerves (3, 4). Because nervous tissue does not spontaneously regenerate like epithelial and connective tissues, injury to the nervous system leaves most patients significantly disabled. Patients and their families urgently seek new treatments and technologies to repair the damaged nervous system and restore lost function.

In the development of new technologies to repair the nervous system, there are two general approaches: guiding axons from the site of injury to the original synaptic site, and implanting neurons to replace neurons lost as a result of injury. In some cases, only axon guidance is necessary in order to restore lost function, which is true (theoretically) for peripheral nerve damage. In other cases, such as spinal cord injury where loss of function is due to loss of neurons and disrupted axons, both approaches are needed. Neurite regeneration may be sufficient to restore function lost from severed axons (5–7), but plasticity of native neurons alone may be insufficient to completely compensate for neurons lost at the injury site (8, 9).

One approach to improve axon regeneration is the design of scaffolds to act as guidance cues for neurites. Our laboratory has helped to pioneer the neurite-guiding potential of electrospun fibers, and we have shown that electrospun fibers serve as physical cues to direct neurite outgrowth from primary neuronal cells (10–15). Electrospinning is a method of producing polymer fibers with diameters on the nanometer to micrometer scale. When aligned, electrospun fibers guide neurite extension parallel to the direction of fiber alignment (16–18). Application of electrospun fibers to *in vivo* models of nerve injury have demonstrated the capability of these acellular scaffolds to promote robust neurite extension (19, 20), and can lead to functional recovery in the spinal cord (21, 22) and peripheral nerve (23–26). Electrospun fibers have also been seeded with cells prior to implantation in the spinal cord (27). However, it can be difficult to get neurons to adhere to electrospun fibers unless adhesion ligands are used. While electrospun fibers are good materials for directing axon extension, they may be inadequate as a platform for implantation of new neurons without further modification.

To address the problem of protecting neurons, glia, and their stem cell precursors on electrospun fibers, we have turned to cell-encapsulating hydrogels. By encapsulating transplanted cells in a hydrogel matrix, we endeavor to provide a protective barrier to shield transplanted cells from toxic environments, ambient air and temperature, and mechanical perturbations during implantation that would otherwise lead to cell harm or detachment (28). A large body of research exists that focuses on the design of hydrogels for use in the

peripheral and central nervous system. However, most engineered hydrogels use crosslinkers, some of which are cytotoxic or produce cytotoxic byproducts. One method of generating cross-linked hydrogels that has received recent attention is through Diels-Alder reactions, which has been used to tune hydrogel mechanical properties (29, 30). Another common is through the use of microwave-assisted crosslinking, which was recently used to add RGD peptides to increase cell adhesion (31). In contrast, hydrogel fibers made by interfacial polyelectrolyte complexation (IPC) form via electrostatic interactions between positively and negatively charged hydrogel solutions (32), so no covalent crosslinks are formed. IPC fibers have been shown to be an encapsulant suitable for many cell types (33), and have been shown to support the differentiation of encapsulated human pluripotent stem cells into mature neurons (34). However, the effect of IPC hydrogel fibers on primary neuron or astrocyte populations has not been reported, and no study has attempted to combine IPC hydrogels with electrospun fibers.

In this study, we encapsulated primary neurons and astrocytes in IPC fibers and combined neurons encapsulated within them with electrospun fibers to take advantage of their neurite guiding capacity. Using a Calcein-AM assay, we evaluated the encapsulation viability of primary cortical neurons and astrocytes in IPC fibers using L929 fibroblasts as a positive control. Our findings confirm that IPC fibers, when formed at near-physiological pH, present a suitable environment for sensitive cell types such as primary neurons. To further assess IPC fibers as an encapsulant for use in nerve regeneration, we assembled a cortical neuron-encapsulating IPC fiber / electrospun nanofiber composite scaffold and explored its capacity for neuritogenesis and neurite elongation. The results of these experiments suggest that IPC fibers may be a promising encapsulant for neural tissue engineering applications, especially when used in combination with electrospun nanofibers.

Methods

All experiments were done in accordance with the Animal Component of Research Protocols (ACORPs #0909–012 and #1506–004) as approved by the Ann Arbor VA Subcommittee on Animal Studies and follow both US and international standards regarding the care and use of animals.

IPC Fiber Formation

IPC fibers are formed via the interfacial interactions between oppositely charged polyelectrolyte solutions. In this study, 2.5% w/v sodium alginate (Sigma, A0682) in sterile H_2O was selected as the negatively charged polyelectrolyte solution. This alginate solution was then paired with one of two positively charged polyelectrolyte solutions: acid-soluble chitosan (AsC) or water-soluble chitosan (WsC). The AsC solution was prepared by dissolving 2% w/v low molecular weight chitosan (Aldrich, 448869, 50–190 kDa) in 0.2 M acetic acid. In an effort to increase pH neutrality and, in effect, cell encapsulation viability, a water-soluble chitosan derivative was later prepared by partially acetylating highly deacetylated chitosan. The acetylation reaction was performed using the method described by Kurita, et al (35). The WsC solution was then prepared by dissolving 2% w/v partially acetylated chitosan in 1x PBS.

To initiate fiber formation, a pair of polyelectrolyte solution droplets were dispensed onto a Pyrex glass surface. Using blunt-tipped forceps, the two droplets were brought into contact and IPC fibers were drawn from the interface. Fig. 1A is a picture of the IPC fiber spinning apparatus, and Fig. 1B is a cartoon illustrating the IPC fiber components and the process of fiber formation. To visualize the interface between the polyelectrolyte solutions, Trypan Blue (Gibco, 15250–061) was added to the alginate, as shown in Fig. 1C.

After initiating fiber formation, the IPC fibers were collected using a rotating spindle apparatus, similar to that shown by Wan, et al. (32). Rather than collect IPC fibers directly on the rotating apparatus, glass coverslips were loaded on the spindle arms to catch the newly formed fibers. Fig. 1D is a transmitted light micrograph of an IPC fiber collected on a glass coverslip. This micrograph reveals the microtopography of IPC fibers, consistent with that previously described (32). Outlined in orange is the nuclear fiber bundle, a collection of tightly complexed fibers formed via the charge-charge interactions between the polyelectrolytes. Outlined in blue is a loosely-complexed bead that has formed around the nuclear fiber bundle. It has been shown that beads form along IPC fibers when the speed at which fibers are drawn exceeds a critical rate (32). We hypothesized that the loosely-complexed hydrogel beads would provide additional protection for encapsulated cells, so we rotated the collection spindle with a tangential velocity of ~2.8 cm/s, a speed that ensured bead formation. To better visualize the nuclear fiber bundle, fluorescein sodium salt (Sigma, 46960) was added to the alginate solution, as shown in Fig. 1E. The fluorescent alginate solution was prepared by dissolving 2% w/v sodium alginate in water containing 2 ug/mL fluorescein sodium salt.

IPC Fiber Diameter Measurement

To measure the diameter of the IPC fibers, transmitted light micrographs were collected from IPC fibers spun onto glass coverslips. Using ImageJ software (36), three distinct measurements were collected: Diameter of the loosely complexed hydrogel beads, diameter of the nuclear fiber bundle contained within the loosely complexed hydrogel beads, and the diameter of the nuclear fiber bundle in the narrow regions between the beads. A minimum of 14 measurements were collected for each measurement type. Results are presented as means +/− 1 standard deviation.

L929 Fibroblast Preparation

L929 fibroblasts were purchased from ATCC and grown on 100 mm diameter tissue culture treated plates (Corning, Inc. 353003) in Dulbecco's Modified Eagle Medium (DMEM, Gibco 11885084) with 10% fetal bovine serum (FBS, Gibco 10438026) and 1% Penicillin-Streptomycin-Neomycin antibiotic mixture (PSN, Gibco 15640055). When the plates reached 80–90% confluence, they were passed either 1:5 every 3–5 days or 1:10 every 7–10 days. L929 fibroblasts used in our experiments ranged from pass 5 to pass 28.

To generate a cell suspension for subsequent encapsulation, the medium from 2–3 confluent plates was aspirated and 3 mL 0.25% trypsin-EDTA (Gibco 25200056) was added to each plate. Plates were incubated for 5–10 minutes, or until cells detached, at which time 3 mL FBS was added to inactivate the trypsin-EDTA. The resulting cell suspension was

centrifuged for 5 minutes at 1000 RPM and the cell pellet was obtained. The pellet was resuspended in 0.25 mL DMEM with 1% PSN and added to 1.75 mL of 2.5% sodium alginate solution.

Astrocyte Preparation

Astrocytes were isolated from E13-E14 Sprague-Dawley rats. Time-pregnant rats were obtained from Envigo (Indianapolis, IN), anesthetized with isoflurane and ketamine/xylazine, and euthanized via intracardiac injection of sodium pentobarbital. Embryos were then removed from the uterus and their spinal cords were harvested for dissociation. Spinal cords were stripped of all membranes, chopped into 1 mm size pieces, and trypsinized for 13 minutes before manual trituration with a fire polished glass Pasteur pipette. The cell solution was suspended over a 9% OptiPrep density gradient (Alere Technologies AS 1114542) in Leibovitz's L-15 medium (Gibco 11415114) and centrifuged for 15 minutes at 2000 RPM from which the cell pellet was obtained. Cells were re-suspended in a plating medium similar to motor neuron medium as described by Leach and colleagues (29–31), excluding 2 mM L-glutamine, and supplemented to 10% FBS. Astrocytes were plated in 100 mm diameter tissue culture-treated plates that had been coated with 3 mL 0.01% poly-L-lysine (PLL, Sigma-Aldrich P4832) for one hour, aspirated, rinsed three times with 5 mL sterile water for 5 minutes, then left at 4°C to dry overnight. Plates were split 1:3 once confluent and passes 3–7 were used to ensure nonspecific cells were not being utilized.

Much like the L929 fibroblast suspensions, astrocyte suspensions were prepared using 2–3 confluent plates. Cell pellets were resuspended in 0.25 mL Hibernate®-E medium (Gibco A12476–01) and then carefully mixed with 1.75 mL 2.5% sodium alginate solution.

Cortical Neuron Preparation

Cortical neurons were isolated from E17 Sprague-Dawley rats. After removing the embryos from the uterus, the heads were decapitated and placed in a tissue culture treated plate with ice cold Neurobasal medium. The meninges were carefully sliced anterior to posterior, freeing the brain and allowing the brain to be dissected and transferred to a plate with cold L-15 medium. All blood vessels and connective membranes were removed. The remaining brain tissue was cut into small 1 mm pieces, transferred to a 50-mL conical, and centrifuged at 1000 RPM for 5 minutes. The supernatant was carefully removed and 3 mL of 0.25% trypsin-EDTA was added to the cell pellet. The conical was placed in a 37°C bead bath for 13 minutes, and then 3 mL of FBS was added to the conical to inactivate the trypsin-EDTA. The conical was then centrifuged at 1000 RPM for 2.5 minutes and supernatant gently removed. A fire-polished glass Pasteur pipette that had been coated on the inside with FBS for 5–10 minutes was used to triturate the cells into 2 mL L-15 medium. Once a homogenous cell suspension was achieved, 48 mL L-15 medium was added to the cell suspension, and the conical was centrifuged at 1000 RPM for 10 minutes. The supernatant was removed and the cells were re-suspended in motor neuron medium, prepared as previously described (12), and plated onto ten 100 mm diameter PLL-coated tissue culture-treated plates in motor neuron medium (12).

Cortical neuron suspensions were prepared using 1–4 plates (~10–40 million cells), depending on the intended use. For viability experiments, lower encapsulation densities were necessary in order to adequately distinguish live and dead cells. For immunolabeling experiments, however, more plates and higher encapsulation densities were able to be used. For all cortical neuron experiments, the cell suspension was prepared by first aspirating the motor neuron media and applying 3 mL of 0.25% trypsin-EDTA to each plate. After 5 minutes of incubation, 3 mL of FBS was added to inactivate the trypsin-EDTA. The cortical neurons were gently agitated by repeatedly pipetting the liquid across the surface of the plate, and the suspension was transferred to an appropriately-sized conical to be centrifuged at 1000 RPM for 5 minutes. Once the supernatant had been removed, the cell pellet was re-suspended in 50 μL of motor neuron medium. 40 uL of the cortical neuron suspension was mixed with 200 uL of 2.5% sodium alginate solution prior to IPC fiber formation.

Calcein-AM Viability Assay

To evaluate cell encapsulation viability, cell-encapsulating IPC fibers were cultured on PLGA-coated glass coverslips and stained with the LIVE/DEAD Viability/Cytotoxicity Kit, for mammalian cells, by Molecular Probes. In some experiments, PDMS inserts were added to the culture wells to keep IPC fibers submerged in culture media and attached to the PLGA-coated glass surface. The green fluorescent calcein-AM and the red fluorescent ethidium homodimer-1 components of the LIVE/DEAD kit were used to identify live and dead cells, respectively. Cells that fluoresced with any green were counted as live and cells that fluoresced only red were counted as dead.

For each cell type, cell-encapsulating IPC fibers formed from alginate and chitosan were evaluated 30 minutes, 4 hours, 1 day, and 7 days post-encapsulation. As a control, ‘pre-encapsulation’ viability was also evaluated by staining cells plated directly onto PLL-coated glass coverslips. For the 30-minute time point, cell-encapsulating IPC fibers were submerged in LIVE/DEAD staining solution immediately after encapsulation, and were incubated for 30 minutes. For all other time points, the cell-encapsulating IPC fibers were incubated in each cell type’s respective culture media until 30 minutes prior to the post-encapsulation timepoint. At that time, the culture media was aspirated and replaced with the LIVE/DEAD staining solution. After 30 minutes of incubation, the cell-encapsulating IPC fibers were imaged immediately after aspirating the stain. Using an EVOS FL imaging system with RFP and GFP light cubes and a 20x objective, a minimum of 20 fluorescence micrographs were collected from each sample. The number of live and dead cells in each micrograph were counted manually, and a percent survival was calculated by summing the live cell counts from each sample’s set of micrographs and dividing by the total number of counted cells. After observing the unhealthy morphologies of cortical neurons encapsulated in IPC fibers formed using AsC, the encapsulation viability of cortical neurons was re-evaluated using WsC as the positively charged polyelectrolyte solution. For statistical analysis, a sample was defined as the collection of 4–6 coverslips loaded onto the collection spindle during a single spin. At least 3 samples were collected for each cell-type/time-point combination. Specific n-values were as follows: Pre-encapsulation (L929 n = 3, Astrocyte n = 4, AsC Neuron n= 7, WsC Neuron n = 4), 30 minutes (L929 n = 8, Astrocyte n = 5, AsC Neuron n = 3, WsC Neuron n = 4), 4 hours (L929 n = 5, Astrocyte n = 5, AsC Neuron n = 4,

WsC Neuron n = 4), 1 day (L929 n = 5, Astrocyte n = 5, AsC Neuron n = 3, WsC Neuron n = 3), and 7 days post-encapsulation (L929 n = 5, Astrocyte n = 5, AsC Neuron n = 3, WsC Neuron n = 3).

Differences between cell types and chitosan formulations were compared using 2-way ANOVA ($\alpha = 0.05$) and Tukey's multiple comparison tests. To make the comparisons fair, pre-encapsulation survival data were omitted from the ANOVA because cells in these groups were never exposed to either polyelectrolyte and therefore to anything in the hydrogel fiber that could decrease their survival.

Collection of Aligned Electrospun Fibers

Aligned electrospun fibers were collected in a fashion similar to that described in previous work (37). In short, a 4% w/v solution of poly-L-lactic acid (PLLA, Evonik Resomer L210) dissolved in a 9:1 mixture of chloroform:dimethylformamide was loaded into a blunted syringe. A voltage of 20 kV was applied to the syringe tip while a syringe pump dispensed electrospinning solution at a rate of 0.20 mL/hr. A collection disk was positioned 30 cm from the syringe tip and rotated at 800 RPM. The voltage of the collection disk was maintained at −2 kV. 6% PLGA-coated glass coverslips were taped onto the disk and electrospun nanofibers were collected for 10 minutes.

Scanning Electron Microscopy

Scanning electron micrographs of electrospun fibers were collected with an AMRAY 1910 field emission scanning electron microscope using SemTech Solutions X-Stream image capture software. Electrospun fiber samples were placed under argon and coated with gold using a Polaron sputter coater. The accelerating voltage was 3kV. A representative image of electrospun fibers is presented in Fig. 2A.

Composite Scaffold Construction

Composite scaffolds were constructed by drawing IPC fibers overtop the aligned electrospun nanofibers. Depending upon how the electrospun nanofiber composites were loaded on the IPC collection spindle, either "parallel" or "perpendicular" composite scaffolds were created. Fig. 2B is a cartoon illustrating the components of the parallel composite. In the parallel composite, the electrospun fiber coverslips were loaded onto the IPC collection spindle such that the IPC nuclear fiber bundle aligned with the underlying electrospun fibers. Fig. 2C is a photograph of a parallel composite where the IPC fibers were dyed with Trypan Blue to help distinguish the composite scaffold components. When perpendicular composites were constructed, the electrospun nanofiber coverslips were rotated 90 degrees such that IPC nuclear fiber bundle ran perpendicular to the electrospun nanofiber bundle.

Immunofluorescence Staining

Immunofluorescent techniques were used to investigate neurite formation and elongation within IPC fibers. In all images shown, cortical neurons encapsulated in IPC fibers were fixed and stained 3 days post-encapsulation. Like the LIVE/DEAD viability experiments, PDMS inserts were sometimes used to prevent IPC fibers from separating from the underlying substrates. After 3 days of incubation, cell-encapsulating IPC fibers were fixed

for 30 minutes in 4% PFA at room temperature. After three 5-minute PBS washes, the samples were permeabilized for 30 minutes in a block/perm solution containing 1.25% Bovine Serum Albumin (Sigma A4503), 0.05% Triton X-100 (Sigma T-9284), and 2% Normal Goat Serum (Gibco 16210–064) in 1xPBS. The samples were then incubated overnight at 20°C in a primary antibody solution containing 1.125% Bovine Serum Albumin, 0.045% Triton X-100, 10% Normal Goat Serum, and monoclonal anti-B-Tubulin III produced in mouse (1:1000 Tuj1, Sigma-Aldrich T8578). The following day, two-three 5–10 minute PBS washes were performed prior to incubating for 2–4 hours at room temperature, protected from light, in a secondary antibody solution containing FITC-conjugated Goat anti-Mouse IgG (1:200, Sigma F0257) in 1x PBS. The PLGA films and overlying fibrous constructs were transferred to a fresh coverslip and mounted on a glass slide in ProLong Gold with DAPI (Life Technologies P36931) after three additional 5–10 minute PBS washes.

Results

Primary Neural Cell Viability in IPC-fibers

We began this study by asking whether IPC fibers composed of alginate and chitosan, demonstrated to be a useful encapsulant of other cell types, could be used to encapsulate primary neurons and glia. Cells from the nervous system have been repeatedly demonstrated to be more difficult to grow than cells from other organ systems. Of the cells within the nervous system, primary neurons from the CNS have been found more difficult to grow than glia. Based on these observations from the field of neuron culture, several straightforward hypotheses can be formulated. First, astrocytes in IPC fibers will not survive as well as a common connective tissue cell type, such as a fibroblast. Second, primary neurons will not survive as well as fibroblasts. Third, primary neurons will not survive as well as astrocytes.

Primary cortical neurons and astrocytes were encapsulated in IPC fibers fabricated using alginate and acid-soluble chitosan (AsC). Cells were assessed for viability at 30 min, 4 h, 1 d, and 7 d. Cells from the line L929, a line of fibroblasts, were used as positive controls.

The sensitivity of primary neurons to in vitro environments suggests also that AsC, having a lower pH outside a typical range found in vivo, would be harsher and therefore more deleterious to survival than water-soluble chitosan (WsC). As a consequence, our fourth hypothesis was that neurons in WsC would survive better than those in AsC, and we encapsulated some neurons in IPC fibers fabricated with WsC to test this.

Results of our experiments can be seen in Fig. 3. Survival percentages of all cell types at each encapsulation (culture) time are graphed in Fig. 3A. Photographs of cells in the IPC fibers can be seen in Fig. 3B–E. Statistical analysis of these data was accomplished with a 2-way ANOVA test in which we included all data except for pre-encapsulation, since cells in these samples were never exposed to the chitosan and alginate hydrogels that compose the IPC fibers.

Cell viability as a function of cell type

We found that cell type and chitosan formulation (referred to hereafter as cell type) produced 41% of the variation of cell survival in IPC fibers ($p < 0.0001$). Multiple comparison testing of survival data by cell type averaged across all encapsulation times in culture showed that L929 fibroblasts (78.9 ± 12.1%; mean ± S.D.) survived better than astrocytes (58.4 ± 13.4%; $p < 0.001$), consistent with our first hypothesis that astrocyte survival would be poorer than that of fibroblasts. We also found that L929 fibroblast survival was superior to that of neurons in fibers fabricated using both AsC (44.2 ± 6.78%; $p < 0.0001$) and WsC (59.9 ± 9.84%; $p < 0.01$), consistent with our second hypothesis that fibroblasts would be more robust than neurons in these IPC fibers.

We also tested whether astrocytes would survive better than neurons. Consistent with our third hypothesis, survival of astrocytes exceeded survival of neurons in fibers fabricated with AsC ($p < 0.05$). However, survival of astrocytes was not statistically different from that of neurons in fibers fabricated with WsC. Additionally, neurons in fibers fabricated with WsC exhibited greater survival than neurons in fibers fabricated with AsC ($p < 0.05$). These last two findings are consistent with our fourth hypothesis, namely that WsC would be superior to AsC in its ability to promote neuron survival.

To understand how different cell types compared to each other over time, multiple comparisons of survival percentages by cell type were performed at each time point. While there exist statistically significant differences in survival among the different cell types at each time, we found no consistent relationship between cell type and viability at the different time points.

Cell viability as a function of time

Since the goal of encapsulating neurons and astrocytes in IPC fibers is to create new constructs by which to tissue engineer the nervous system after injury, adequate survival of neurons and glial cells at time periods of weeks to months is vital. And because ex vivo environments can be challenging to cells, we also hypothesized that cell survival would decrease over time, and that the survival percentages of the most vulnerable of the cell types, neurons, would have the greatest decrease in survival over time, most easily observed at the 7-day time point.

The 2-way ANOVA test also revealed that time in culture explained only 5.0% of the variation in cell survival (n.s.), but that interaction between cell type and time was explained 18% of the variation ($p < 0.01$). To explain this interaction, we broke down survival to examine cell survival changes over time. Multiple comparisons of survival percentages at the different time points were performed within each cell type. In contrast to our hypothesis that neuronal survival would decrease over the 1 week of culture, no significant differences in survival percentage were observed between any of the time points, either for neurons in AsC fibers or for neurons in WsC fibers. Similarly, in contrast to our hypothesis that astrocyte survival might also decrease over time, we found that the percentage of live astrocytes actually increased between 30 min and 7 d ($p < 0.01$). Similar to astrocytes, the percentage

of viable L929 fibroblasts also increased over time; a statistically significant increase in survival was observed at 1 d ($p < 0.01$) and 7d ($p < 0.05$) compared to 30 min.

Neuron Morphology and Neuritogenesis

One of the hallmarks of neurons is their morphology, characterized by the presence of neurites. Classified as axons and dendrites, neurites are the processes by which neurons connect with one another and through which information flows to other neurons. Any biomaterial construct that impedes formation of neurites will fail in its utility as a tool in neural tissue engineering.

We noted that primary cortical neurons encapsulated in IPC fibers formed using AsC failed to present neurites (Fig. 3D). Since a lack neuritogenesis could be an indication of poor neuronal health, we hypothesized that the low pH inherent in AsC impeded neurite formation, and that replacing it with WsC could allow neurons to form neurites. In the experiments to assess viability above, we noticed that aligned processes could be seen in neurons encapsulated in IPC fibers fabricated using WsC (Fig. 3E).

To test this further, we compared neurite formation in IPC fabricated with AsC vs. WsC. Neurons in IPC were stained with the neuron-specific β-tubulin marker, Tuj1. Immunofluorescent labelling revealed primary cortical neurons encapsulated in IPC fibers fabricated using AsC presented few, if any, neurites (Fig. 4A), while those encapsulated in IPC fibers formed using WsC presented many neurites that were aligned (Fig. 4B). We also found that the neurites that formed in the IPC fibers fabricated with WsC were highly aligned. These findings were demonstrated in several replications of these experiments. Based on these observations, we conclude that IPC fibers fabricated using WsC are more conducive to neurite formation than those fabricated using AsC.

Neuron Behavior in IPC Fiber / Electrospun Fiber Composite Scaffolds

One of the original purposes of the study was to determine if these IPC fibers could be used to encapsulate cells from the nervous system around electrospun fibers. Therefore, our final step was to determine whether neurons encapsulated in these composite scaffolds would extend processes along electrospun fibers. To test this, composite scaffolds were created by drawing cortical neuron-encapsulating IPC fibers on top of a bundle of aligned electrospun fibers. Because the hydrogel fibers fabricated by IPC contain smaller component fibers, it can be difficult to distinguish whether these or electrospun fibers are responsible for neurite guidance. In order to help determine this, two variants of the composite scaffold were constructed: parallel composites, in which the IPC fibers are aligned parallel to the electrospun fibers in the bundle, and perpendicular composites, in which the IPC fibers are oriented perpendicular to the electrospun fiber bundle. Some of the composite scaffolds were constructed using IPC fabricated with AsC (Fig. 5A); most were constructed using IPC fabricated with WsC (Fig. 5B–D).

We first hypothesized that the topographical cues of the electrospun fibers in these composite fibers would provide directional guidance to neurons and help initiate neurite formation in IPC fibers fabricated with AsC. In these parallel composites (Fig. 5A), neuritogenesis remained severely stunted, despite the presence of electrospun fibers. When

parallel composites were constructed using WsC-IPC fibers, we observed robust neurite elongation (Fig. 5B). We also observed that compared to the neurites near the nuclear fiber bundle, some neurites in the beaded regions of the IPC fibers were seen more clearly in the focal plane of the electrospun fiber bundle. These neurons exhibited neurite outgrowth parallel to the alignment of the electrospun fibers in a region where nuclear fibers were sparse, suggesting orientation by electrospun fibers.

To better visualize the unique contributions to unilateral alignment provided by the two scaffold components, perpendicular composite scaffolds were fabricated with neurons in WsC. We hypothesized that, in this configuration, we would be able to better distinguish which neurons in the composite scaffold were following electrospun fiber cues and which were following cues from the IPC nuclear fiber bundle. To determine the extent of influence of each fiber type on neurite alignment, perpendicular composite scaffolds were fabricated with neurons in WsC. We found that some neurites did extend along the underlying electrospun fibers, perpendicular to the IPC nuclear bundle, suggesting that the addition of electrospun fibers to a cell-encapsulating IPC fiber construct can result in additional guidance of aligned neurite elongation. Neurites following IPC fibers (Fig. 5C) were noticeably separated from neurites following electrospun fibers (Fig. 5D), suggesting that the IPC and electrospun fibers were not sufficiently integrated.

IPC Fiber Morphology

The narrowest portions of the IPC nuclear fiber bundle, located in the regions between the loosely complexed hydrogel beads, measured to be 40.6 +/− 29.4 um for IPC fibers formed using ASC and 35.9 +/− 27.8 um for IPC fibers formed using WSC. The widest portions of the IPC nuclear fiber bundle, located within the loosely complexed hydrogel beads, measured 225.5 +/− 59.7 um using ASC and 188.9 +/− 42.0 um using WSC. The diameters of the hydrogel beads themselves were measured to be 572.2 +/− 159.8 um and 465.1 +/− 106.7 um when formed using ASC and WSC, respectively.

Discussion

Our primary objective in this study was to investigate the suitability of hydrogels made by IPC as an encapsulant for neural cells to be seeded on electrospun fibers. Using IPC fibers, we investigated viability of neurons and astrocytes, the effects of material composition on neuritogenesis and neurite extension, and whether IPC fibers integrated well with electrospun fibers when fabricated on electrospun fiber bundles. In this study, we found that primary neuron and astrocyte survival averaged 59.9 % and 58.4 %, respectively, over the whole study. At 7 d, the longest time point of our study, neuron and astrocyte survival averaged 46.7 % and 74.3 %, respectively. We observed that primary neurons can effectively extend neurites in IPC fibers composed of alginate and water-soluble chitosan (WsC) but not acid-soluble chitosan. Lastly, we found that in the composite scaffolds, neurites oriented to either the nuclear fibers or electrospun fibers at different focal planes, suggesting IPC fibers did not integrate with electrospun fibers as well as we had anticipated.

In our testing of cell viability, we found that neurons survive more poorly than astrocytes and that astrocytes survive more poorly than fibroblasts. This was completely expected. IPC

fibers have been used to encapsulate epithelial and connective tissue types with ease (38). However, neurons in vitro are more difficult to grow than and appear to have a special vulnerability relative to other primary cell types, so it is unwarranted to merely apply IPC methods to neurons and expect them to survive without difficulty.

One reason that neurons may not have performed as well as astrocytes and fibroblasts in IPC fibers may stem from the polyelectrolytes that compose them, chitosan and alginate. Cells have been found to reside primarily in the beads of alginate that span the nuclear fiber core. Alginate is negatively charged which decreases cell-to-material adhesion, while chitosan is positively charged, which increases it (39). Since the survival of neurons in vitro is highly dependent on positive charge of the substratum to promote neuronal adhesion and neuritogenesis (40), we hypothesized that survival of neurons encapsulated in the alginate beads may be poor. However, others have found that primary neurons encapsulated in hydrogels, including alginate, have survived at percentages comparable to or greater than ours. Perale found that astrocytes and glial cell lines survival at 55% in a hydrogel of agarose and carbomer, but do not specify culture duration (41). Zhou and colleagues found that 50% of neurons and glia survived on the surfaces of poly(MAETAC-PEGMA) hydrogels with tethered acetylcholine (42). Alginate has also been found to be a suitable hydrogel for primary neurons, producing survivals of 83% in ultrasoft alginate (43) and 70–80% in alginate-carboxymethyl cellulose doped with ECM proteins (44). In our experiments, many neurons were able to contact the outer fibrils and the nuclear core, as evidenced by the neurite extension observed in the IPC fibers. These chitosan-containing structures could have acted as positively-charged substrates inside the surrounding alginate environment, thus supporting neuronal adhesion and survival.

We also found that neuron survival did not change over time. We suspect that neuron survival did not decrease after the 30-minute time point because after the traumatic process of encapsulation, little additional trauma was incurred. Encapsulated neurons did not increase, because those harvested from E17 rats are essentially mature and therefore do not proliferate. Additionally, there was a decrease in neuronal survival by day 7. This decrease is likely due to the long-term culture of the neurons. Longer-term culture of primary neurons is difficult and depends upon culture conditions, including optimal media and cell density (45). Encapsulation of both neurons and glia together would be one of several long term solutions to this problem. In contrast to neurons, both astrocytes and fibroblasts increased over time, suggesting proliferation after having been encapsulated. Both were encapsulated from serum-containing media, which promotes proliferation.

We found that AsC impairs neuritogenesis and that WsC allows neurite guidance. This is not surprising, since cells from the central nervous system are known to be sensitive to acidic pH (2, 4). We suspect that the aligned fibrils contained in the IPC nuclear fiber bundle are the most likely source of directed neurite growth, working by contact guidance. We further suspect that the positive change of the chitosan is attractive to the cell bodies and the neurites, and assists in attracting neurites to the fibrils and longitudinal nuclear core, facilitating the guided neurite growth through the IPC hydrogel fibers. The fact that all the chitosan in the IPC fibers collects in the nuclear core or the nuclear fibrils scattered

throughout the alginate beads (32) supports this idea. More work should be done to confirm the mechanisms involved in the direction of IPC fiber-guided neurite extension.

We found that the IPC fiber components did not merge with the electrospun fiber bundle as cohesively we had anticipated. This is despite the fact that the beads of the IPC fibers appeared to spread out on electrospun fiber bundles (Figs. 1 and 2). However, the spatial separation between composite scaffold components likely limits the opportunity for cooperativity between the different directional guidance cues. Based on neurites visualized in composite scaffolds where the electrospun fiber bundles were perpendicular to the IPC fibers, it appeared that some of the neurons appeared to escape or de-encapsulate from the bead components of the IPC fibers. From our results, it is clear that both electrospun fibers and the fibrils / nuclear core contained within the IPC fibers are capable of orienting neurites. The lack of integration between IPC and electrospun fibers suggests that more sophisticated approaches will be needed to successfully encapsulate electrospun fibers and cells into an IPC construct.

Survival of neurons in the 50% range suggests that improvements to long term viability could be made by doping or functionalizing the alginate with ECM glycoproteins (e.g., laminin or fibronectin) or trophic factors appropriate to the neuronal phenotype of interest. Increasing the density of neurons and neural stem cells to be encapsulated should also improve viability, as could co-encapsulation of neurons with astrocytes or Schwann cells. We believe that we have demonstrated that water soluble chitosan should be used when attempting to encapsulate neurons in IPC hydrogels. We also hypothesize that there are other approaches that will successfully allow combining hydrogel structures fabricated with IPC technology to encapsulate neural cells on electrospun fibers.

In these experiments, we have shown that unilateral neurite elongation can be supported in the absence of electrospun fibers. However, using other approaches, the incorporation of electrospun fibers may still be advantageous to maximize guidance in scaffolds for neural repair. Because nerve regeneration and spinal cord repair are long-term processes, an effective neurite guidance scaffold should be able to provide sustained directional support over weeks to months. The in vivo degradation of IPC fibers has not yet been well-characterized, but the degradation rates of other hydrogels suggest that the direction cues provided by IPC fibers may not be sufficiently sustained over these long times. It is possible, on the other hand, to engineer electrospun fibers with slowly degrading polymers which should facilitate continued guidance no matter how fast IPC fibers degrade. In summary, we do foresee a future in which IPC hydrogel structures can be used to encapsulate electrospun fibers and neural cells to create effective scaffolds for neural repair.

Acknowledgements

The authors wish to thank the staff of the Microscopy & Image Analysis Laboratory at the University of Michigan for the use of their facilities for SEM of the electrospun fibers. We are grateful to the Undergraduate Research Opportunity Program at the University of Michigan whose student researchers have become regular personnel in our laboratory. We also wish to thank the following funding agencies for their support of this work and our personnel: VA Rehab R&D (I21-RX001904) the National Institute of Dental and Craniofacial Research at NIH (2 T32 DE007057-40), and the Department of Defense (W91ZSQ2136N601).

References

1. Bruns J, Hauser WA. The Epidemiology of Traumatic Brain Injury: A Review. Epilepsia. 2003;44:2–10. doi: 10.1046/j.1528-1157.44.s10.3.x.
2. Spinal cord injury facts and figures at a glance. J Spinal Cord Med. 2014;37(5):659–60. doi: 10.1179/1079026814z.000000000341. [PubMed: 25229744]
3. Asplund M, Nilsson M, Jacobsson A, Holst Hv. Incidence of Traumatic Peripheral Nerve Injuries and Amputations in Sweden between 1998 and 2006. NED. 2009;32(3):217–28. doi: 10.1159/000197900.
4. Taylor CA, Braza D, Rice JB, Dillingham T. The Incidence of Peripheral Nerve Injury in Extremity Trauma. American Journal of Physical Medicine & Rehabilitation. 2008;87(5):381–5. doi: 10.1097/PHM.0b013e31815e6370. [PubMed: 18334923]
5. Houle JD, Tom VJ, Mayes D, Wagoner G, Phillips N, Silver J. Combining an Autologous Peripheral Nervous System "Bridge" and Matrix Modification by Chondroitinase Allows Robust, Functional Regeneration beyond a Hemisection Lesion of the Adult Rat Spinal Cord. J Neurosci. 2006;26(28):7405–15. doi: 10.1523/jneurosci.1166-06.2006. [PubMed: 16837588]
6. Alilain WJ, Horn KP, Hu H, Dick TE, Silver J. Functional regeneration of respiratory pathways after spinal cord injury. Nature. 2011;475(7355):196–200. doi: 10.1038/nature10199. [PubMed: 21753849]
7. Lee Y-S, Lin C-Y, Jiang H-H, DePaul M, Lin VW, Silver J. Nerve Regeneration Restores Supraspinal Control of Bladder Function after Complete Spinal Cord Injury. J Neurosci. 2013;33(26):10591–606. doi: 10.1523/jneurosci.1116-12.2013. [PubMed: 23804083]
8. Navarro X, Vivó M, Valero-Cabré A. Neural plasticity after peripheral nerve injury and regeneration. Progress in Neurobiology. 2007;82(4):163–201. doi: 10.1016/j.pneurobio.2007.06.005. [PubMed: 17643733]
9. Raineteau O, Schwab ME. Plasticity of motor systems after incomplete spinal cord injury. Nature Reviews Neuroscience. 2001;2(4):263–73. doi: 10.1038/35067570. [PubMed: 11283749]
10. Corey JM, Lin DY, Mycek KB, Chen Q, Samuel S, Feldman EL, et al. Aligned electrospun nanofibers specify the direction of dorsal root ganglia neurite growth. Journal of biomedical materials research Part A. 2007;83(3):636–45. [PubMed: 17508416]
11. Purcell EK, Naim Y, Yang A, Leach MK, Velkey JM, Duncan RK, et al. Combining Topographical and Genetic Cues to Promote Neuronal Fate Specification in Stem Cells. Biomacromolecules. 2012;13(11):3427–38. doi: Doi 10.1021/Bm301220k. [PubMed: 23098293]
12. Leach MK, Feng ZQ, Gertz CC, Tuck SJ, Regan TM, Naim Y, et al. The culture of primary motor and sensory neurons in defined media on electrospun poly-L-lactide nanofiber scaffolds. J Vis Exp 2011(48). Epub 2011/03/05. doi: 10.3791/23892389 [pii].
13. Gertz CC, Leach MK, Birrell LK, Martin DC, Feldman EL, Corey JM. Accelerated neuritogenesis and maturation of primary spinal motor neurons in response to nanofibers. Dev Neurobiol. 2010;70(8):589–603. Epub 2010/03/10. doi: 10.1002/dneu.20792 [doi]. [PubMed: 20213755]
14. Corey JM, Gertz CC, Wang BS, Birrell LK, Johnson SL, Martin DC, et al. The design of electrospun PLLA nanofiber scaffolds compatible with serum-free growth of primary motor and sensory neurons. Acta Biomater. 2008;4(4):863–75. [PubMed: 18396117]
15. Feng ZQ, Wu JH, Cho WR, Leach MK, Franz EW, Naim YI, et al. Highly aligned poly(3,4-ethylene dioxythiophene) (PEDOT) nano- and microscale fibers and tubes. Polymer. 2013;54(2):702–8. doi: DOI 10.1016/j.polymer.2012.10.057. [PubMed: 25678719]
16. Wang HB, Mullins ME, Cregg JM, Hurtado A, Oudega M, Trombley MT, et al. Creation of highly aligned electrospun poly-L-lactic acid fibers for nerve regeneration applications. Journal of Neural Engineering. 2009;6:016001. doi: 10.1088/1741-2560/6/1/016001. [PubMed: 19104139]
17. Lee Y-S, Livingston Arinzeh T. Electrospun Nanofibrous Materials for Neural Tissue Engineering. Polymers. 2011;3(1):413–26. doi: 10.3390/polym3010413.
18. Schaub NJ, Johnson CD, Cooper B, Gilbert RJ. Electrospun Fibers for Spinal Cord Injury Research and Regeneration. J Neurotrauma. 2015;33(15):1405–15. doi: 10.1089/neu.2015.4165.
19. Hurtado A, Cregg JM, Wang HB, Wendell DF, Oudega M, Gilbert RJ, et al. Robust CNS regeneration after complete spinal cord transection using aligned poly-l-lactic acid microfibers.

Biomaterials. 2011;32(26):6068–79. doi: 10.1016/j.biomaterials.2011.05.006. [PubMed: 21636129]

20. Yu W, Zhao W, Zhu C, Zhang X, Ye D, Zhang W, et al. Sciatic nerve regeneration in rats by a promising electrospun collagen/poly(epsilon-caprolactone) nerve conduit with tailored degradation rate. BMC Neuroscience. 2011;12(1):68. doi: 10.1186/1471-2202-12-68. [PubMed: 21756368]
21. Zamani F, Tehran MA, Latifi M, Shokrgozar MA, Zaminy A. Promotion of spinal cord axon regeneration by 3D nanofibrous core-sheath scaffolds. Journal of Biomedical Materials Research Part A. 2013;00A:000–. doi: 10.1002/jbm.a.34703.
22. Gelain F, Panseri S, Antonini S, Cunha C, Donega M, Lowery J, et al. Transplantation of Nanostructured Composite Scaffolds Results in the Regeneration of Chronically Injured Spinal Cords. ACS nano. 2011;5(1):227–36. doi: 10.1021/nn102461w. [PubMed: 21189038]
23. Jiang X, Mi R, Hoke A, Chew SY. Nanofibrous nerve conduit-enhanced peripheral nerve regeneration. Journal of Tissue Engineering and Regenerative Medicine. 2014;8(5):377–85. doi: 10.1002/term.1531. [PubMed: 22700359]
24. Panseri S, Cunha C, Lowery J, Del Carro U, Taraballi F, Amadio S, et al. Electrospun micro- and nanofiber tubes for functional nervous regeneration in sciatic nerve transections. BMC Biotechnol. 2008;8:39. doi: 10.1186/1472-6750-8-39. [PubMed: 18405347]
25. Neal RA, Tholpady SS, Foley PL, Swami N, Ogle RC, Botchwey EA. Alignment and composition of laminin–polycaprolactone nanofiber blends enhance peripheral nerve regeneration. Journal of Biomedical Materials Research Part A. 2012;100A(2):406–23. doi: 10.1002/jbm.a.33204.
26. Chew SY, Mi R, Hoke A, Leong KW. Aligned Protein-Polymer Composite Fibers Enhance Nerve Regeneration: A Potential Tissue-Engineering Platform. Advanced Functional Materials. 2007;17(8):1288–96. doi: 10.1002/adfm.200600441. [PubMed: 18618021]
27. Liu C, Huang Y, Pang M, Yang Y, Li S, Liu L, et al. Tissue-Engineered Regeneration of Completely Transected Spinal Cord Using Induced Neural Stem Cells and Gelatin-Electrospun Poly (Lactide-Co-Glycolide)/Polyethylene Glycol Scaffolds. PloS one. 2015;10(3):e0117709. doi: 10.1371/journal.pone.0117709. [PubMed: 25803031]
28. Hackelberg S, Tuck SJ, He L, Rastogi A, White C, Liu L, et al. Nanofibrous scaffolds for the guidance of stem cell-derived neurons for auditory nerve regeneration. PloS one. 2017;12(7):e0180427. doi: 10.1371/journal.pone.0180427. [PubMed: 28672008]
29. Li S, Wang L, Yu X, Wang C, Wang Z. Synthesis and characterization of a novel double cross-linked hydrogel based on Diels-Alder click reaction and coordination bonding. Materials Science and Engineering: C. 2018;82:299–309. doi: 10.1016/j.msec.2017.08.031. [PubMed: 29025662]
30. Baker AEG, Tam RY, Shoichet MS. Independently Tuning the Biochemical and Mechanical Properties of 3D Hyaluronan-Based Hydrogels with Oxime and Diels–Alder Chemistry to Culture Breast Cancer Spheroids. Biomacromolecules. 2017;18(12):4373–84. doi: 10.1021/acs.biomac.7b01422. [PubMed: 29040808]
31. Mauri E, Sacchetti A, Vicario N, Peruzzotti-Jametti L, Rossi F, Pluchino S. Evaluation of RGD functionalization in hybrid hydrogels as 3D neural stem cell culture systems. Biomaterials science. 2018;6(3):501–10. Epub 2018/01/26. doi: 10.1039/c7bm01056g. [PubMed: 29368775]
32. Wan ACA, Liao IC, Yim EKF, Leong KW. Mechanism of fiber formation by interfacial polyelectrolyte complexation. Macromolecules. 2004;37(18):7019–25. doi: 10.1021/ma0498868.
33. Wan ACA, Cutiongco MFA, Tai BCU, Leong MF, Lu HF, Yim EKF. Fibers by interfacial polyelectrolyte complexation – processes, materials and applications. Materials Today. 2016;19(8):437–50. doi: 10.1016/j.mattod.2016.01.017.
34. Lu HF, Lim S-X, Leong MF, Narayanan K, Toh RPK, Gao S, et al. Efficient neuronal differentiation and maturation of human pluripotent stem cells encapsulated in 3D microfibrous scaffolds. Biomaterials. 2012;33(36):9179–87. doi: 10.1016/j.biomaterials.2012.09.006. [PubMed: 22998816]
35. Kurita K, Koyama Y, Nishimura S-i, Kamiya M. Facile Preparation of Water-Soluble Chitin from Chitosan. Chemistry Letters. 1989;18(9):1597–8. doi: 10.1246/cl.1989.1597.
36. Rueden CT, Schindelin J, Hiner MC, DeZonia BE, Walter AE, Arena ET, et al. ImageJ2: ImageJ for the next generation of scientific image data. BMC Bioinformatics. 2017;18(1):529. doi: 10.1186/s12859-017-1934-z. [PubMed: 29187165]

37. Tuck SJ, Leach MK, Feng ZQ, Corey JM. Critical variables in the alignment of electrospun PLLA nanofibers. Mat Sci Eng C-Mater. 2012;32(7):1779–84. doi: 10.1016/j.msec.2012.04.060.

38. Leong MF, Toh JK, Du C, Narayanan K, Lu HF, Lim TC, et al. Patterned prevascularised tissue constructs by assembly of polyelectrolyte hydrogel fibres. Nature communications. 2013;4:2353 Epub 2013/08/21. doi: 10.1038/ncomms3353.

39. Nisbet DR, Moses D, Gengenbach TR, Forsythe JS, Finkelstein DI, Horne MK. Enhancing neurite outgrowth from primary neurones and neural stem cells using thermoresponsive hydrogel scaffolds for the repair of spinal cord injury. Journal of Biomedical Materials Research Part A. 2009;89A(1):24–35. doi: 10.1002/jbm.a.31962.

40. Corey JM, Wheeler BC, Brewer GJ. Micrometer resolution silane-based patterning of hippocampal neurons: critical variables in photoresist and laser ablation processes for substrate fabrication. IEEE Trans Biomed Eng. 1996;43(9):944–55. [PubMed: 9214810]

41. Perale G, Giordano C, Bianco F, Rossi F, Tunesi M, Daniele F, et al. Hydrogel for cell housing in the brain and in the spinal cord. The International Journal of Artificial Organs. 2011;34(3):295–303. doi: 10.5301/ijao.2011.6488. [PubMed: 21445832]

42. Zhou Z, Yu P, Geller HM, Ober CK. The role of hydrogels with tethered acetylcholine functionality on the adhesion and viability of hippocampal neurons and glial cells. Biomaterials. 2012;33(8):2473–81. doi: 10.1016/j.biomaterials.2011.12.005. [PubMed: 22196899]

43. Palazzolo Gemma BN, Cenciarelli Orlando, Dermutz Harald, and Zenobi-Wong Marcy. Ultrasoft Alginate Hydrogels Support Long-Term Three-Dimensional Functional Neuronal Networks. Tissue Engineering Part A. 2015;21(15–16):2177–85. Epub May 19, 2015. doi: 10.1089/ten.tea.2014.0518. [PubMed: 25915796]

44. Beduer A, Braschler T, Peric O, Fantner GE, Mosser S, Fraering PC, et al. A compressible scaffold for minimally invasive delivery of large intact neuronal networks. Adv Healthc Mater. 2015;4(2):301–12. Epub 2014/09/03. doi: 10.1002/adhm.201400250. [PubMed: 25178838]

45. Brewer GJ, Torricelli JR, Evege EK, Price PJ. Optimized survival of hippocampal neurons in B27-supplemented Neurobasal, a new serum-free medium combination. J Neurosci Res. 1993;35(5):567–76. [PubMed: 8377226]

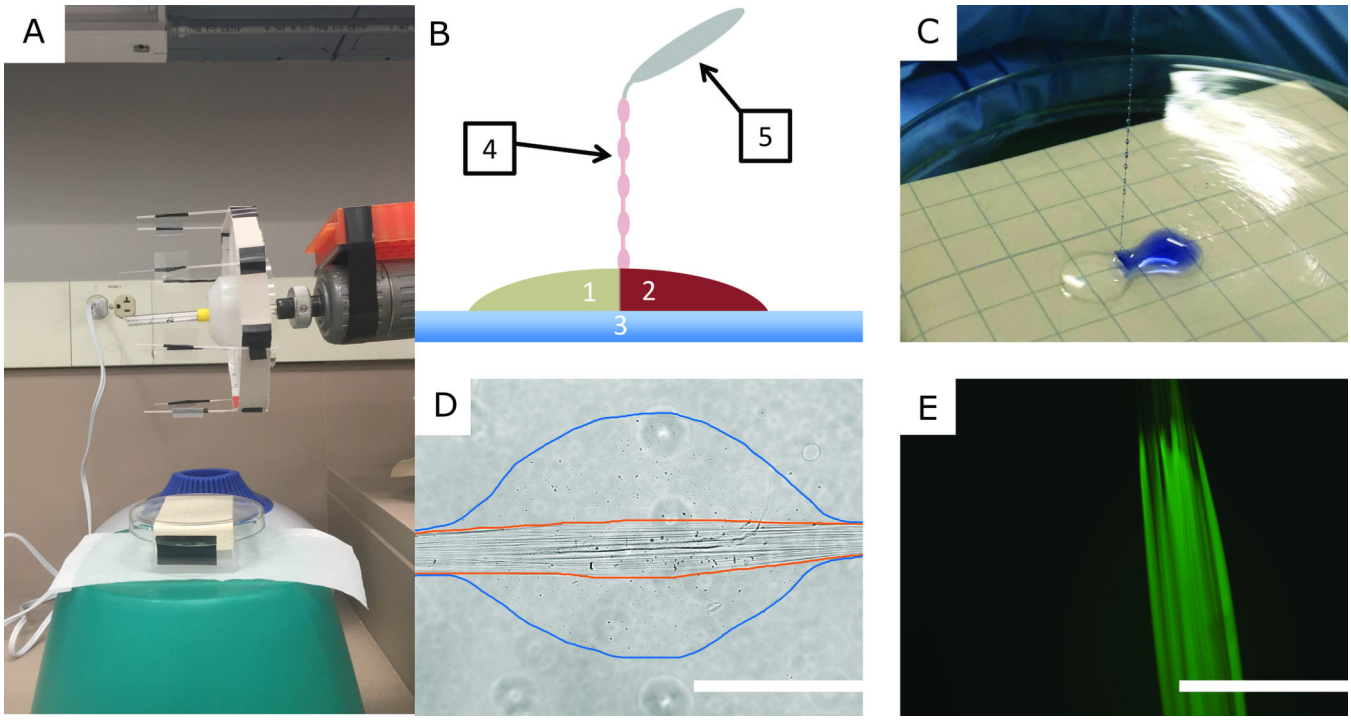

Figure 1.

IPC Fiber Formation and Characterization. A. A picture of the IPC-fiber spinning apparatus. B. Cartoon showing IPC fiber formation: Oppositely charged polyelectrolyte solutions (1,2) are brought together on a glass surface (3). An IPC fiber (4) is drawn by grasping the interface with forceps (5) and pulling upward. C. Photograph of IPC fiber formation using an alginate solution dyed with Trepan Blue. D. Transmitted light micrograph of an IPC fiber. The nuclear fiber bundle is outlined in orange and the loosely complexed hydrogel bead is outlined in blue. E. Fluorescence micrograph of an IPC fiber formed using an alginate solution dyed with fluorescein sodium salt. Scale bars: 400 μm.

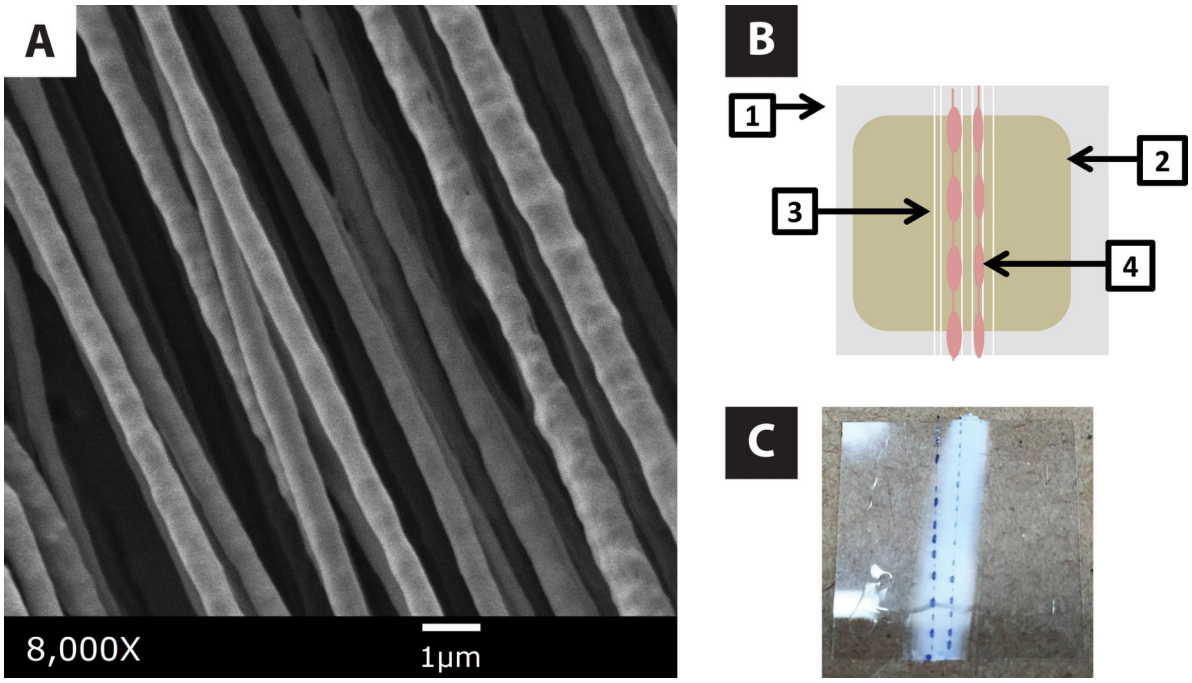

Figure 2.

Electrospun Nanofiber Composite Scaffold Construction. A. SEM photomicrograph of aligned nanofibers electrospun from a 4% PLLA solution in chloroform. B. Cartoon of the parallel composite construct: glass coverslip (1), 6% PLGA solvent cast (2), aligned electrospun fiber bundle (3), cell-encapsulating IPC fibers (4). C. Photograph of a partial parallel composite scaffold containing IPC fibers formed using an alginate solution dyed with Trypan Blue.

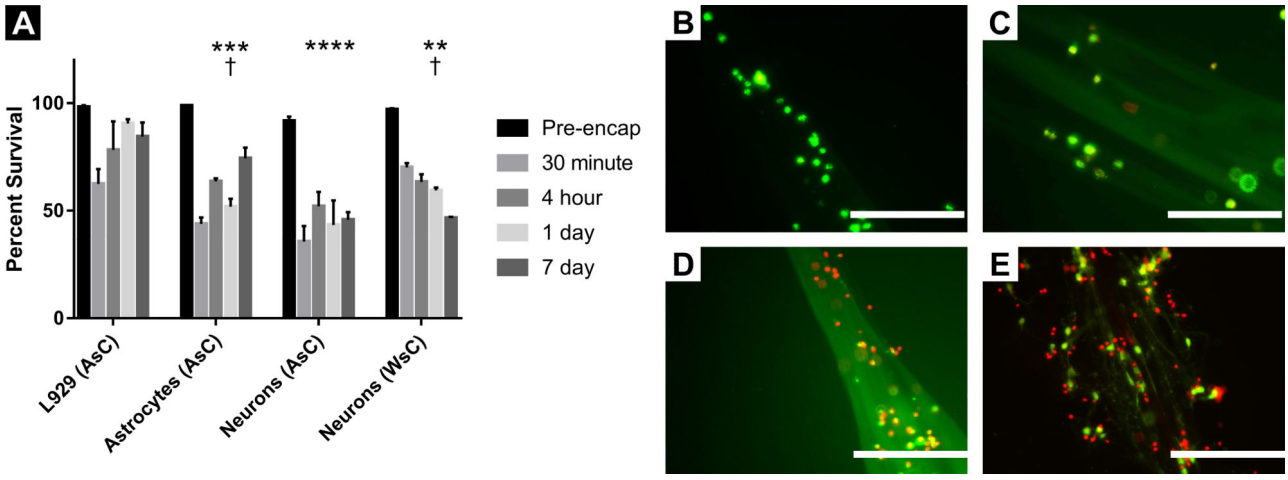

Figure 3.

Viability of Cell-Encapsulating IPC Fibers. A. Survival percentages calculated using the Live/Dead Viability Assay. L929 fibroblasts, primary astrocytes, primary cortical neurons using AsC, and primary cortical neurons using WsC were evaluated at the following durations of encapsulation: Pre-encapsulation, 30 minutes, 4 hours, 1 day, and 7 days post-encapsulation. Technical and biological replicates for each group varied, but all groups were repeated at least three times (see materials and methods for specific values). Data are plotted as mean ± S.E.M. **, $p < 0.01$; ***, $p < 0.001$; ****, p, 0.0001; compared to mean L929 survival. †, $p < 0.05$, compared to mean Neuron (AsC) survival. B-E. Representative micrographs of live and dead cells 7 days post-encapsulation. L929 fibroblasts (B), primary astrocytes (C), primary cortical neurons in IPC fibers formed using AsC (D), primary cortical neurons in IPC fibers formed using WsC (E). Scale bars: 200 μm.

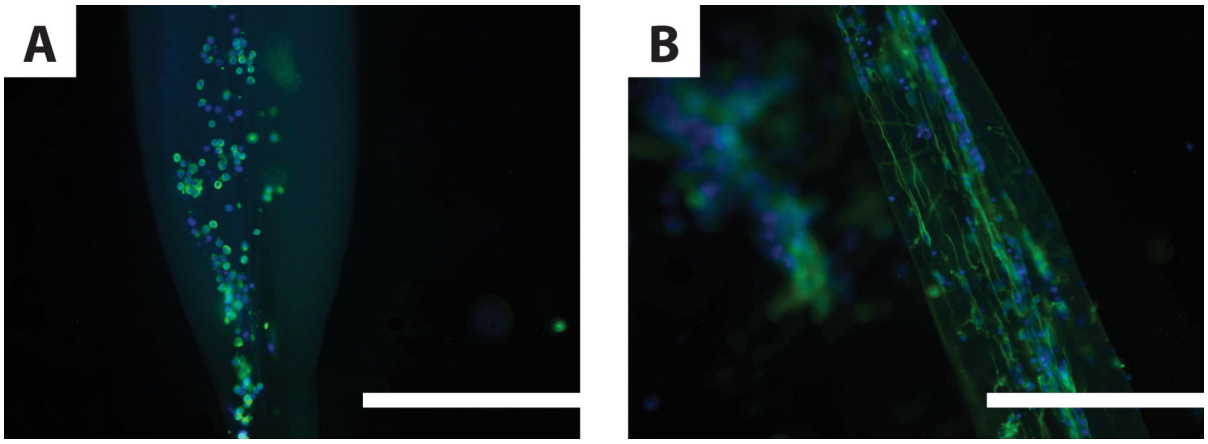

Figure 4.

Neurite Elongation in IPC Fibers. Immunofluorescent micrographs of primary cortical neurons 3 days post-encapsulation in IPC fibers. Neurons are labeled with the neuron-specific marker tubulin-Tuj1 (green) and cell nuclei with DAPI (blue). A. Cortical neurons in IPC formed using AsC did not present neurites. B. Cortical neurons in IPC fibers formed using WsC presented neurites that elongated along the length of the nuclear fiber bundle. Similar images were collected from preparations in at least one other separate trial. Scale bars are 200 μm.

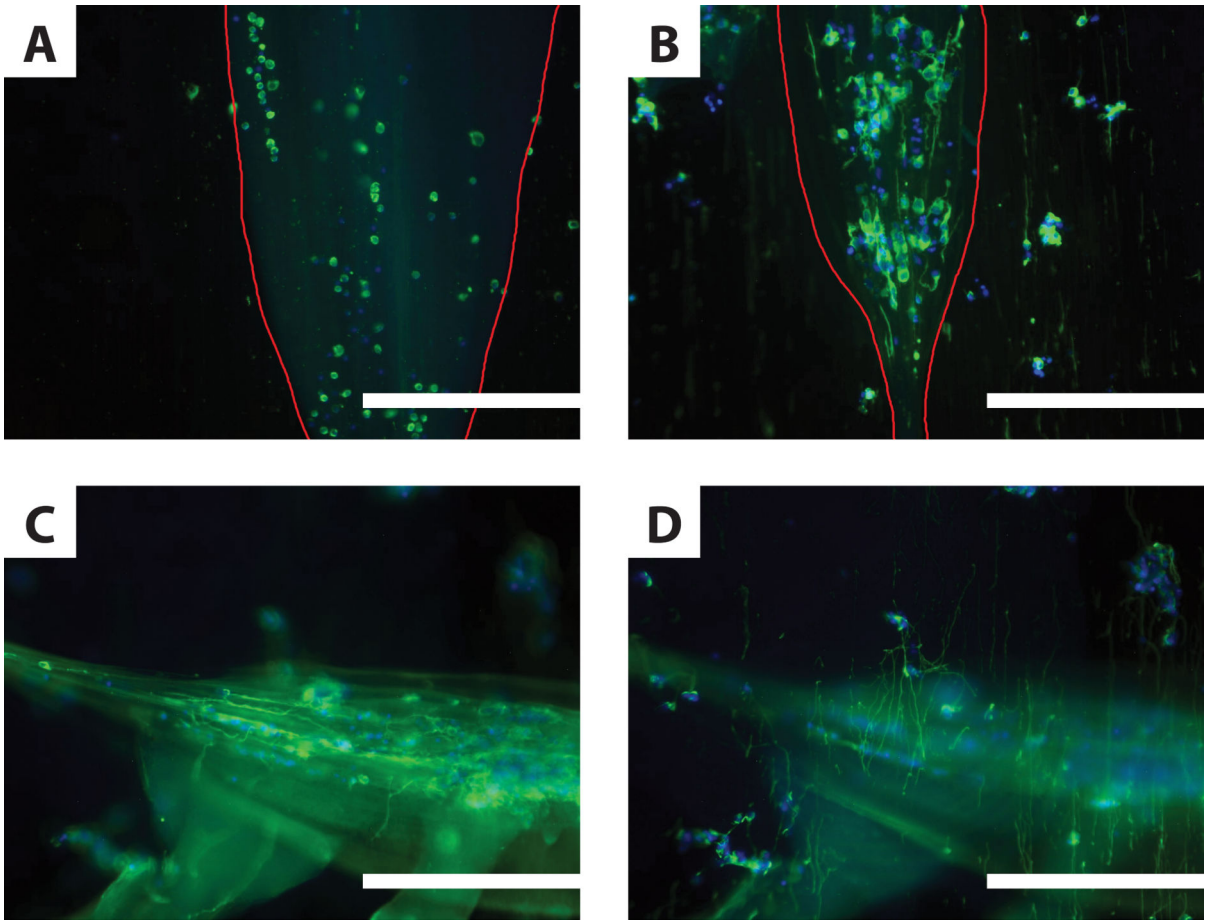

Figure 5.

Neurite Elongation in Composite Scaffolds. Immunofluorescent micrographs of primary cortical neurons 3 days post-encapsulation in IPC fiber / electrospun fiber composite scaffolds. Neurons are labeled with the neuron-specific marker tubulin-Tuj1 (green) and cell nuclei with DAPI (blue). A-B. Parallel composite scaffolds, where cell-encapsulating IPC fibers (outlined in red) were drawn such that the nuclear fiber bundle shared the same orientation as the underlying electrospun fibers. When IPC fibers were made using AsC (A), no neurites formed. When IPC fibers were made using WsC (B), encapsulated cells extended neurites unilaterally, as did de-encapsulated cells in contact with electrospun fibers. C-D. Two different focal planes of the same perpendicular composite scaffold containing IPC fibers formed using WsC (n = 3). Cells encapsulated in IPC fibers extend neurites horizontally, along the length of the nuclear fiber bundle (C). Neurites also extend vertically, along the underlying electrospun fiber mat (D). Similar images were collected from preparations in at least one other separate trial. Scale bars: 200 μm.